Hyperpolarized butyrate: A metabolic probe of short chain fatty acid metabolism in the heart

Ball, DR, Rowlands, B, Dodd, MS, Le Page, L, Ball, V, Carr, CA, Clarke, K & Tyler, DJ

DOI 10.1002/mrm.24849
ISSN 0740-3194

Publisher: Wiley

Hyperpolarized Butyrate: A Metabolic Probe of Short Chain Fatty Acid Metabolism in the Heart

Daniel R. Ball, Ben Rowlands, Michael S. Dodd, Lydia Le Page, Vicky Ball, Carolyn A. Carr, Kieran Clarke, and Damian J. Tyler*

Purpose: Butyrate, a short chain fatty acid, was studied as a novel hyperpolarized substrate for use in dynamic nuclear polarization enhanced magnetic resonance spectroscopy experiments, to define the pathways of short chain fatty acid and ketone body metabolism in real time.

Methods: Butyrate was polarized via the dynamic nuclear polarization process and subsequently dissolved to generate an injectable metabolic substrate. Metabolism was initially assessed in the isolated perfused rat heart, followed by evaluation in the in vivo rat heart.

Results: Hyperpolarized butyrate was generated with a polarization level of 7% and was shown to have a T_1 relaxation time of 20 s. These physical characteristics were sufficient to enable assessment of multiple steps in its metabolism, with the ketone body acetoacetate and several tricarboxylic acid cycle intermediates observed both in vitro and in vivo. Metabolite to butyrate ratios of 0.1–0.4% and 0.5–2% were observed in vitro and in vivo respectively, similar to levels previously observed with hyperpolarized [2-^{13}C]pyruvate.

Conclusions: In this study, butyrate has been demonstrated to be a suitable hyperpolarized substrate capable of revealing multi-step metabolism in dynamic nuclear polarization experiments and providing information on the metabolism of fatty acids not currently achievable with other hyperpolarized substrates. **Magn Reson Med 71:1663–1669, 2014. © 2013 Wiley Periodicals, Inc.**

Key words: dynamic nuclear polarization; butyrate; hyperpolarization; magnetic resonance spectroscopy; short chain fatty acids; ketone bodies; heart

Dynamic nuclear polarization (DNP) is a technique that allows the low sensitivity of magnetic resonance spectroscopy to be overcome by inducing high nuclear polarization of ^{13}C substrates at low temperatures in the solid state (1). Using a rapid dissolution process, this high polarization can be briefly maintained in the liquid state at room temperature (2,3), which has important implications for the study of metabolism as key metabolic substrates can be polarized (4–8). Following injection of hyperpolarized substrates, direct metabolic information can be obtained both in vivo and ex vivo (9–16). The enzymatic conversion of hyperpolarized substrates can be observed, as can kinetic parameters of such conversions (17,18).

To date, studies using dynamic nuclear polarization to define metabolic pathways have focused extensively on pyruvate, which allows assessment of carbohydrate metabolism (7,8). Pyruvate has also been used indirectly as a measure of fatty acid oxidation by looking at the reduction in pyruvate dehydrogenase (PDH) flux seen when fatty acids are supplied (13). Some research has been directed toward alternative substrates to reveal other aspects of metabolism including amino acid metabolism, tricarboxylic acid (TCA) cycle reactions, and intracellular redox potential (4–6,19,20). Hyperpolarized acetate has also been used as a marker of fatty acid metabolism, via its conversion to acetylcarnitine (21), however, it bypasses the β-oxidation pathway and lacks the ability to reveal information on ketone body metabolism due to its short carbon chain length.

Butyrate, a four-carbon fatty acid, has the potential to enable assessment of short chain fatty acid (SCFA) metabolism, as its low molecular weight and carboxyl carbon should ensure suitable polarization properties (i.e., high nuclear polarization and long T_1 relaxation time) (15). In human metabolism, along with acetate and propionate, butyrate is produced in the gut as a result of digestion of insoluble plant matter (e.g., cellulose) by intestinal microflora (22). Butyrate is the primary fuel of choice for colonocytes (23) and a large body of research is focused on attenuating and preventing colon cancer (24,25). Butyrate is taken up into cells via the monocarboxylate transporter enzyme (26), where previous ^{13}C and radiolabeled studies have shown that it is metabolized to the ketone bodies, acetoacetyl-CoA, and β-hydroxybutryl-CoA (27,28) (Fig. 1). These can either be metabolized further, via acetyl-CoA in the TCA cycle, or be exported to muscle tissue. In situations in which the diet is particularly high in fiber, and therefore insoluble plant matter, small concentrations of butyrate can be found in the blood stream (29), where it can be metabolized by muscle tissues, such as the heart.

In diabetes, there is an increase in the production of ketone bodies due to upregulation of the ketogenic enzymes, which catalyze the steps leading to the formation of acetoacetate and β-hydroxybutyrate (30). Using hyperpolarized butyrate it may be possible to investigate aspects of ketone body metabolism and to determine the extent to which enzymes relevant to the production and use of ketone bodies are altered in diabetes. In addition,

Cardiac Metabolism Research Group, Department of Physiology, Anatomy & Genetics, University of Oxford, Oxford, UK.

Grant sponsor: Medical Research Council, British Heart Foundation and Oxford Instruments Molecular Biotools.

*Correspondence to: Damian Tyler, Ph.D., Department of Physiology, Anatomy & Genetics, Sherrington Building, University of Oxford, Parks Road, Oxford, UK. E-mail: damian.tyler@dpag.ox.ac.uk

Received 1 March 2013; revised 25 April 2013; accepted 28 May 2013

DOI 10.1002/mrm.24849

Published online 24 June 2013 in Wiley Online Library (wileyonlinelibrary.com).

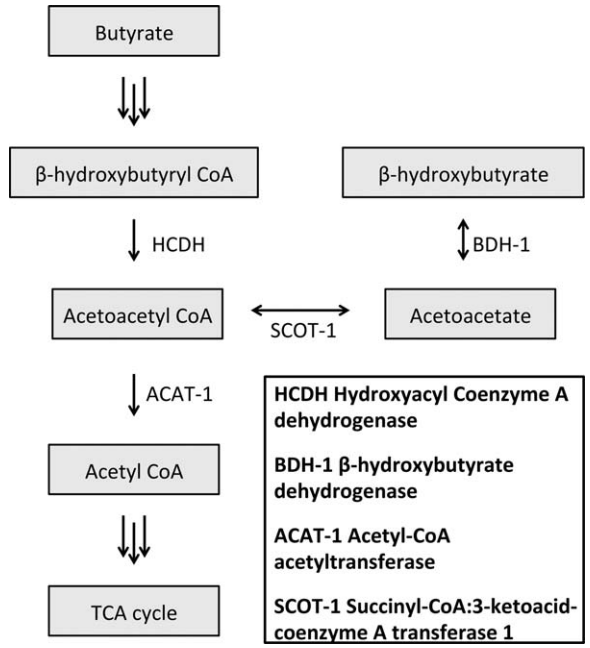

FIG. 1. Expected metabolic pathway for butyrate in the heart. The injected [1-^{13}C]butyrate should be converted into β-hydroxybutyryl-CoA and acetoacetyl-CoA before subsequent conversion into either the ketone bodies (acetoacetate and β-hydroxybutyrate) or acetyl-CoA (for entry into the TCA cycle).

changes in SCFA metabolism could also be observed using the metabolic pathway steps upstream of ketone body synthesis.

The aim of this study was to characterize the properties of butyrate as a metabolic substrate and to assess its suitability in hyperpolarization experiments, both ex vivo and in vivo. The heart was chosen as the target organ to ascertain the potential of butyrate as a hyperpolarized substrate because cardiac muscle is capable of using a wide range of metabolic substrates (31), has a high metabolic demand and, under normal conditions, uses mostly fatty acids (32,33). It should therefore metabolize butyrate rapidly whilst sustaining normal cardiac function.

METHODS

All chemicals were purchased from Sigma-Aldrich (Gillingham, Dorset, UK) and used as supplied unless stated.

Butyric Acid Preparation

To 21.9 mg [1-^{13}C]butyric acid was added 0.44 mg OX063 (Oxford Instruments, Abingdon, UK), followed by 4 μL dimethyl sulfoxide, and 3 μL of a 1:50 dilution of Dotarem (Guerbet, France) made up with double distilled water. The mixture was then vortexed briefly. This was loaded directly into a sample cup, and polarized using either a HyperSense hyperpolarizer (Oxford Instruments, Abingdon, UK) for ex vivo work or a previously described prototype polarizer (GE Healthcare, Amersham, UK) for in vivo work (2). Polarization was performed for approximately 1 h, at a magnetic field strength of 3.35 T and a microwave power level of 100 mW. Dissolution was carried out using 6 mL of buffer containing NaOH (40 mM), ethylenediaminetetraacetic acid (0.3 mM), and Trizma base (40 mM), to yield a solution with a pH of 7.4 and a sodium butyrate concentration of ~40 mM.

Polarization and T_1 Measurement

A dual tuned ^{13}C/^{1}H probe (M2M Imaging, Cleveland, OH) was used in combination with a vertical bore 11.7 T magnet (Magnex Scientific, Oxford, UK) and a Bruker console (Bruker Biospin GmbH, Ettlingen, Germany) running Paravision 2.1.1 and XWinNMR 2.6. Once butyrate polarization and dissolution was complete, 2 mL of the hyperpolarized liquid was withdrawn and injected into a 20-mm test tube ($n = 3$), previously placed in the ^{13}C/^{1}H probe, and a ^{13}C pulse-acquire sequence initiated [averages = 1, 4096 pts, sweep width (SW) = 180.693 ppm, repetition time (TR) = 1 s with 20 acquisitions at each of the following pulse lengths: 25, 50, and 75 μs]. The signal amplitudes in the acquired spectra were fitted in the time domain using the AMARES algorithm in the jMRUI software package (34,35). The T_1 was calculated by fitting the measured signal decay to an exponential decay curve, using the variable pulse lengths to fit and correct for the effects of radio frequency (RF) excitation. The liquid state nuclear polarization was measured by comparison of the amplitude of the first point of the T_1 decay curve with a subsequently acquired thermal polarization acquisition [TR = 300 s, averages = 24, flip angle (FA) = 90°].

Isolated Heart Perfusion

Male Wistar rats (BW ~300 g, Harlan, UK) were anaesthetized with 140 mg kg^{-1} pentabarbitone. The hearts were then excised and briefly washed in ice-cold Krebs Henseleit (KH) buffer, followed by dissection to reveal the aorta. The aorta was cannulated, tied off with 3/0 suture (Pearsalls, UK), and the heart perfused in the Langendorff mode (36) at 85 mmHg pressure, using KH buffer at a temperature of 37°C and oxygenated with 95%O_2/5%CO_2 gas (37–40).

A polyethylene tube was inserted into the left ventricle and through the apex of the heart, in order to drain Thebesian flow. A polypropylene balloon connected to a pressure transducer and a PowerLab system (AD Instruments, Abingdon, UK) was then inserted into the left ventricle to monitor contractile function. The heart was then placed inside a 20 mm NMR test tube, and the tube inserted into the bore of the 11.7 T magnet described above.

Assessment of Butyrate Metabolism in the Perfused Heart

Hearts from male Wistar rats ($n = 5$) were initially perfused with KH buffer containing butyrate (4 mM) and glucose (10 mM). A hyperpolarized [1-^{13}C]butyrate dissolution was carried out and the hyperpolarized butyrate added to a chamber containing oxygenated KH buffer containing only glucose. This generated a KH buffer that matched the buffer initially supplied to the perfused heart (i.e., 10 mM glucose, 4 mM butyrate). The supply

to the perfused heart was subsequently switched to the hyperpolarized butyrate solution and a ^{13}C pulse-acquire experiment immediately started (TR = 1 s, FA = 30°, SW = 180 ppm, 4096 pts). A fully relaxed ^{31}P scan (TR = 15 s, FA = 90°, averages = 40, SW = 49.39 ppm, 2048 pts), followed by a series of rapid ^{31}P scans (TR = 0.25 s, FA = 30°, averages = 120, SW = 49.39 ppm, 2048 pts, 100 measurements) were then performed. Twenty minutes into this series of rapid scans, the buffer was changed to one containing KH with 4 mM butyrate and either 0.0, 2.5, or 10 mM glucose. A second hyperpolarized [1-^{13}C]butyrate dissolution and acquisition was then carried out, followed finally by another fully relaxed ^{31}P acquisition.

Effect of Butyrate on Carbohydrate Metabolism

The effect of butyrate on carbohydrate metabolism was also assessed using hyperpolarized [1-^{13}C]pyruvate (8). The hearts ($n = 5$) were initially perfused with KH containing 2.5 mM pyruvate alone. A hyperpolarized [1-^{13}C]pyruvate dissolution was carried out as previously described (16), followed by a fully relaxed ^{31}P scan, and a series of rapid ^{31}P scans (as described above). The buffer was then changed to KH with 2.5 mM pyruvate and 4 mM butyrate, and the scans repeated. This was followed by a final buffer change to KH containing 4 mM butyrate alone, and a final [1-^{13}C]pyruvate dissolution performed.

In Vivo Assessment of Butyrate Metabolism

A sample of [1-^{13}C]butyric acid was inserted into the prototype polarizer and hyperpolarized for 1 h. Male Wistar rats ($n = 6$, BW ~300 g) were kept in a 12-h light/dark cycle, and were fasted from 17:00 h the evening prior to scanning, thus inducing a fasted metabolic state. The same animals were then scanned a minimum of 48 h later, with no fasting, to generate a fed metabolic state. Male Wistar rats were anaesthetized with 2% isoflurane in oxygen, followed by insertion of a tail vein catheter. They were then placed into a home built cradle, and were heated to ensure a core body temperature of 37°C (41,42). Electrocardiogram (ECG) leads were attached and a respiration loop fitted, with continuous monitoring of heart and respiration rate for the duration of the experiment (43). The rats were placed such that their chest was located directly over a small home built 20 mm diameter ^{13}C RF butterfly surface coil (44). The cradle, holding the anaesthetized rat, was placed into the bore of a 7 T horizontal scanner, connected to a Varian DirectDrive console (Oxford, UK). Localization of the heart was confirmed by acquisition of a proton axial image [echo time (TE) = 1.17 ms, TR = 2.33 ms, matrix size = 64 × 64, field of view (FOV) = 60 mm × 60mm, slice thickness = 2.5 mm, FA = 15°], and shimming was performed to reduce the proton linewidth to < 200 Hz (45). Immediately prior to the injection of the hyperpolarized sample into the rat, an ECG-gated ^{13}C pulse-acquire sequence (TR = 1 s, FA = 5°, SW = 6000 Hz, 2048 pts, 60 measurements) was started, and 1 mL of hyperpolarized [1-^{13}C]sodium butyrate solution was injected for 10 s into the rat, via the tail vein catheter. The remaining hyperpolarized solution was injected into a homebuilt polarimeter to measure polarization.

^{13}C Data Analysis

All acquired ^{13}C data were summed over 30 spectra from the first spectrum in which hyperpolarized [1-^{13}C]butyrate could be clearly observed. Summed spectra were fitted using the AMARES algorithm in the jMRUI software package (34,35) and the fitted metabolite amplitudes were subsequently normalized to the [1-^{13}C]butyrate amplitude (46).

NMR Peak Assignment

A male Wistar rat heart was perfused in the Langendorff mode under constant flow (15 mL min^{-1}) with KH buffer containing 4 mM sodium butyrate, at 37°C gassed with 95%O_2/5%CO_2. After a 10-min equilibration period, the buffer was switched to KH buffer containing 4 mM [1-^{13}C]sodium butyrate and recirculated for 50 min. The heart was then freeze clamped directly on the cannula, and stored at −80°C until needed. Metabolite isolation was performed using a methanol:chloroform extraction described previously (47), using 500 mg of tissue. The extract was reconstituted in 400 μL deuterated phosphate buffer at pH 7.4, before being transferred to a 5 mm NMR tube for analysis. A Bruker AVANCE DPX 300 MHz system was used for all scans, which were run as follows: ^{1}H acquisition (FA = 30°, SW = 4789.27 Hz, averages = 16, 16,834 pts), ^{13}C acquisition (FA = 30°, SW = 17,985.61 Hz, averages = 9500, 32,768 pts, WALTZ16 decoupling), 2D heteronuclear multiple-bond correlation spectroscopy acquisition for $^{1}H/^{13}C$ (SW = 2625.84 Hz/16,762.14 Hz, averages = 256, 2048 pts/1024 pts). Data were processed using ACD/NMR 12.0 (ACD Labs, Toronto, Canada).

Statistical Methods

All data are given as mean ± standard error. Statistical significances between groups were assessed using analysis of variance followed by a paired Student's *t*-test. Statistical significance was considered at $P < 0.05$.

RESULTS

Hyperpolarization of [1-^{13}C]butyric acid provided a liquid state polarization of 7 ± 2%. The T_1 was measured to be 20 ± 1 s. Hyperpolarized butyrate was formulated so that a high concentration of the substrate (~40 mM) was produced upon dissolution for physiological studies.

Spectra from rat hearts perfused with hyperpolarized butyrate had a series of peaks (Fig. 2), which were identified using the high-resolution 2D-NMR data and with reference to literature (7). The spectra demonstrated multistep metabolism, revealing the ketone bodies, acetoacetate, and β-hydroxybutyrate, as well as the TCA cycle related intermediates, citrate, glutamate, and acetylcarnitine.

The metabolism of hyperpolarized [1-^{13}C]butyrate was then determined when co-infused with different concentrations of glucose. No significant differences were

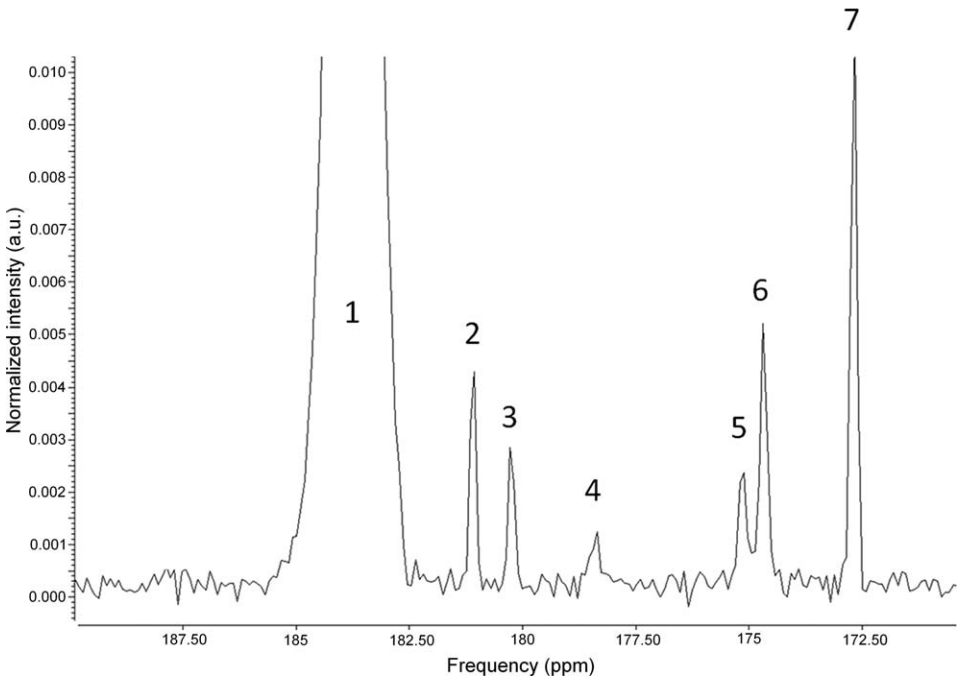

FIG. 2. Hyperpolarized [1-^{13}C] butyrate metabolism in the perfused heart. The peaks shown are (1) butyrate (184 ppm), (2) glutamate (181.16 ppm), (3) β-hydroxybutyrate (180.1 ppm), (4) citrate (178.43 ppm), (5) unknown (175 ppm), (6) acetoacetate (174.6 ppm), and (7) acetylcarnitine (172.6 ppm).

observed between any of the metabolites at any of the glucose concentrations investigated (Fig. 3a) indicating that the glucose concentration did not alter the metabolism of hyperpolarized butyrate. In addition, no significant differences in heart rate, contractile function, or high-energy phosphorus metabolites, as measured by ^{31}P spectroscopy, were seen at any of the glucose concentrations studied.

The effect of butyrate on carbohydrate metabolism was subsequently studied. PDH flux (the sum of bicarbonate and CO_2 signals) was assessed using hyperpolarized [1-^{13}C]pyruvate. Compared to perfusion with pyruvate alone, butyrate significantly decreased PDH flux ($P^* < 0.05$), both when the heart was supplied with a combination of butyrate and pyruvate and when supplied with butyrate alone (Fig. 3b).

The spectra acquired in vivo (Fig. 4) revealed a series of peaks, similar to those seen in the isolated perfused heart. However, the linewidths were significantly broader owing to cardiac and respiratory motion. No differences were seen between the observed metabolites in either the fed or the fasted state (Fig. 5) with respect to [1-^{13}C]butyrate metabolism.

DISCUSSION

In this work, it has been demonstrated that the sensitivity enhancement achieved through the use of

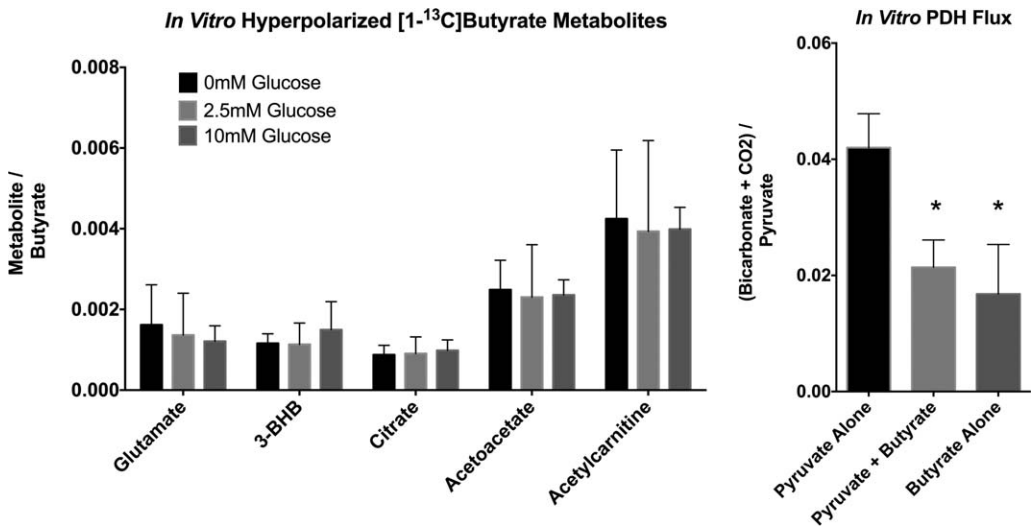

FIG. 3. **a**: The variation in [1-^{13}C]butyrate metabolism with differing glucose concentrations (0, 2.5, and 10 mM). **b**: The change in PDH flux as measured by hyperpolarized [1-^{13}C]pyruvate, when using Krebs Henseleit (KH) buffer with different combinations of 2.5 mM pyruvate (PA) and 4 mM butyrate (BA). *Denotes $P < 0.05$.

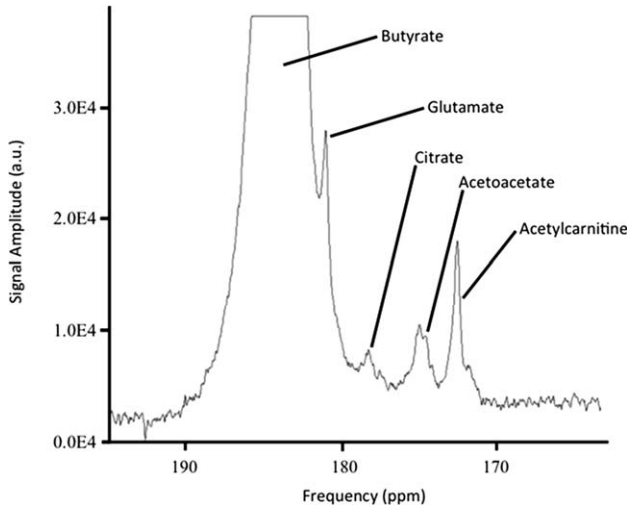

FIG. 4. Hyperpolarized [1-^{13}C]butyrate metabolism in vivo. The peaks shown are butyrate (184 ppm), glutamate (181.16 ppm), citrate (178.43 ppm), acetoacetate (174.6 ppm), and acetylcarnitine (172.6 ppm).

hyperpolarized [1-^{13}C]butyrate in both the perfused and in vivo rat heart was sufficient to obtain high quality spectra. The acquired spectra revealed conversion of the butyrate into multiple downstream metabolites, with sufficient spectral quality to enable quantification of the summed spectra. The exception to this was in vivo β-hydroxybutyrate, which on occasion had too low an signal to noise ratio to be reliably quantified.

The measured physical characteristics of butyrate suggested that it would make a suitable dynamic nuclear polarization substrate for metabolic work. The polarization of [1-^{13}C]butyrate (7%) was lower than that of [1-^{13}C]pyruvate (20–40%) (7,8), but was similar to that of other recently reported hyperpolarized substrates, such as bicarbonate (16%), dehydroascorbic acid (5.9–8.2%), and glucose (4.2%) (4,19,20,48). Hyperpolarized [1-^{13}C]butyrate possessed a sufficiently high T_1 (20 s) to allow observation of metabolism over a prolonged period of time (>60 s), which was again similar to other recently reported hyperpolarized substrates such as bicarbonate (10.1 s), dehydroascorbic acid (20.5 s), and glucose (~10 s) (4,19,20,48).

A key feature of the use of [1-^{13}C]butyrate as a metabolic substrate was the ability to view multistep metabolism, which allowed more information to be extracted from a single experiment (i.e., assessment of SCFA and ketone body metabolism). This feature is particularly important in the perfused heart, where hearts remain stable for relatively short periods (~2 h). In terms of in vivo work, the aim should always be to minimize the number of experiments carried out per animal and maximize the information obtained; and in both cases, a substrate that can reveal multistep/multi-pathway metabolism fulfils these criteria.

The data exploring the alteration in PDH flux when the perfused heart was supplied with butyrate in addition to pyruvate showed changes consistent with those described by Randle and coworkers (49), in that there was significant substrate competition between the carbohydrate, pyruvate, and the fatty acid, butyrate. This alteration will have been mediated via an increase in acetyl-CoA and NADH production from fatty acid oxidation, which inhibits the PDH enzyme, and therefore pyruvate metabolism. Functional data and ^{31}P spectroscopy did not reveal any significant effects caused by the supply of 4 mM butyrate, indicating that the perfused heart can maintain adequate function and energetics when solely supplied with butyrate as a fuel source.

In comparison, the reverse experiment looking at the metabolism of [1-^{13}C]butyrate with varying concentrations of glucose did not reveal any significant metabolic changes. This finding is in agreement with the work of Merritt et al. and Moreno et al., who also showed that the metabolism of glucose (and pyruvate) in the perfused heart could be strongly inhibited by the supply of high concentrations of fatty acids (13,50). A similar inhibition may also explain the findings in the in vivo experiments on fed and fasted states. It is possible that the high concentration of [1-^{13}C]butyrate used in these experiments (1 mL of 40 mM sodium [1-^{13}C]butyrate) may have offered a saturating concentration of fatty acid. The lack of any metabolic alteration between the fed and fasted states may also be related to the fact that the metabolism of short-chain fatty acids lies outside of the normal regulatory mechanisms of fatty acid oxidation (51). Oxidation of long-chain fatty acids is controlled at the point of mitochondrial uptake, via inhibition of carnitine palmitoyltransferase I by malonyl-CoA, whereas SCFAs do not require this mitochondrial transport mechanism and are therefore not regulated in the same way (40).

However, in pathological conditions, such as diabetes, where fatty acid and ketone body metabolism are significantly altered, the use of hyperpolarized [1-^{13}C]butyrate may provide a unique substrate with which to investigate in vivo changes in metabolism and potentially their response to novel therapies. In addition, owing to the importance of butyrate as a fuel for colonocytes, hyperpolarized [1-^{13}C]butyrate may also reveal early metabolic disturbances of the colon, perhaps in advance of the development of cancers.

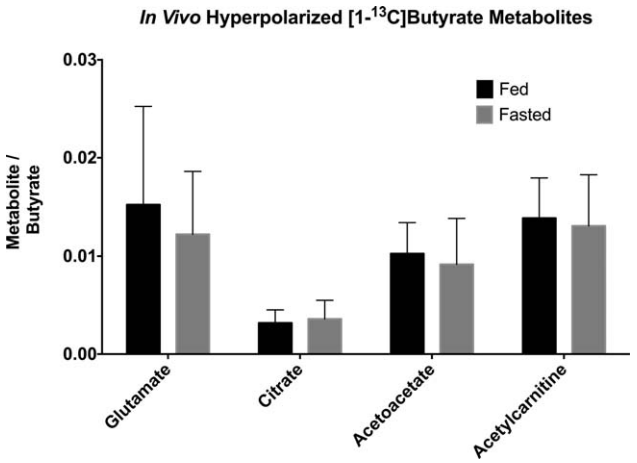

FIG. 5. In vivo metabolism of hyperpolarized [1-^{13}C]butyrate revealed no significant differences between the fed and the fasted states.

CONCLUSIONS

This study has shown that [1-^{13}C]butyrate can be polarized to a level (7%) sufficient to allow use in both perfused heart and in in vivo metabolic experiments. The T_1 (20 s), the rapid uptake and the multistep metabolism make it a suitable substrate to yield information on the metabolism of both SCFAs and ketone bodies. PDH flux data also confirms the expected behavior of adding a SCFA to the cardiac substrate supply. The in vivo hyperpolarized [1-^{13}C]butyrate data, as well as demonstrating no negative effects following injection of [1-^{13}C]butyrate, confirmed the feasibility of using this substrate routinely in vivo.

ACKNOWLEDGMENT

Authors would like to thank Dr. Tim Claridge, at the University of Oxford, Department of Chemistry for his invaluable assistance with the NMR.

REFERENCES

1. Borghini M, Udo F. Dynamic polarization of C-13 nuclei in 1-butanol. Phys Lett A 1973;43:93–94.
2. Ardenkjaer-Larsen JH, Fridlund B, Gram A, Hansson G, Hansson L, Lerche MH, Servin R, Thaning M, Golman K. Increase in signal-to-noise ratio of > 10,000 times in liquid-state NMR. Proc Natl Acad Sci USA 2003;100:10158–10163.
3. Comment A, van den Brandt B, Uffmann K, Kurdzesau F, Jannin S, Konter JA, Hautle P, Wenckebach WTH, Gruetter R, van der Klink JJ. Design and performance of a DNP prepolarizer coupled to a rodent MRI scanner. Concept Magn Reson B 2007;31:255–269.
4. Gallagher FA, Kettunen MI, Day SE, et al. Magnetic resonance imaging of pH in vivo using hyperpolarized 13C-labelled bicarbonate. Nature 2008;453:940–943.
5. Gallagher FA, Kettunen MI, Day SE, Lerche M, Brindle KM. 13C MR spectroscopy measurements of glutaminase activity in human hepatocellular carcinoma cells using hyperpolarized 13C-labeled glutamine. Magn Reson Med 2008;60:253–257.
6. Gallagher FA, Kettunen MI, Hu DE, et al. Production of hyperpolarized [1,4–13C2]malate from [1,4–13C2]fumarate is a marker of cell necrosis and treatment response in tumors. Proc Natl Acad Sci USA 2009;106:19801–19806.
7. Schroeder MA, Atherton HJ, Ball DR, Cole MA, Heather LC, Griffin JL, Clarke K, Radda GK, Tyler DJ. Real-time assessment of Krebs cycle metabolism using hyperpolarized 13C magnetic resonance spectroscopy. FASEB J 2009;23:2529–2538.
8. Schroeder MA, Cochlin LE, Heather LC, Clarke K, Radda GK, Tyler DJ. In vivo assessment of pyruvate dehydrogenase flux in the heart using hyperpolarized carbon-13 magnetic resonance. Proc Natl Acad Sci USA 2008;105:12051–12056.
9. Atherton HJ, Dodd MS, Heather LC, Schroeder MA, Griffin JL, Radda GK, Clarke K, Tyler DJ. Role of pyruvate dehydrogenase inhibition in the development of hypertrophy in the hyperthyroid rat heart: a combined magnetic resonance imaging and hyperpolarized magnetic resonance spectroscopy study. Circulation 2011;123:2552–2561.
10. Day SE, Kettunen MI, Gallagher FA, Hu DE, Lerche M, Wolber J, Golman K, Ardenkjaer-Larsen JH, Brindle KM. Detecting tumor response to treatment using hyperpolarized 13C magnetic resonance imaging and spectroscopy. Nat Med 2007;13:1382–1387.
11. Dodd MS, Ball DR, Schroeder MA, et al. In vivo alterations in cardiac metabolism and function in the spontaneously hypertensive rat heart. Cardiovasc Res 2012;95:69–76.
12. Merritt ME, Harrison C, Sherry AD, Malloy CR, Burgess SC. Flux through hepatic pyruvate carboxylase and phosphoenolpyruvate carboxykinase detected by hyperpolarized 13C magnetic resonance. Proc Natl Acad Sci USA 2011;108:19084–19089.
13. Merritt ME, Harrison C, Storey C, Jeffrey FM, Sherry AD, Malloy CR. Hyperpolarized 13C allows a direct measure of flux through a single enzyme-catalyzed step by NMR. Proc Natl Acad Sci USA 2007;104:19773–19777.
14. Schroeder MA, Atherton HJ, Dodd MS, Lee P, Cochlin LE, Radda GK, Clarke K, Tyler DJ. The cycling of acetyl-coenzyme A through acetylcarnitine buffers cardiac substrate supply: a hyperpolarized 13C magnetic resonance study. Circ Cardiovasc Imaging 2012;5:201–209.
15. Schroeder MA, Clarke K, Neubauer S, Tyler DJ. Hyperpolarized magnetic resonance: a novel technique for the in vivo assessment of cardiovascular disease. Circulation 2011;124:1580–1594.
16. Schroeder MA, Swietach P, Atherton HJ, Gallagher FA, Lee P, Radda GK, Clarke K, Tyler DJ. Measuring intracellular pH in the heart using hyperpolarized carbon dioxide and bicarbonate: a 13C and 31P magnetic resonance spectroscopy study. Cardiovasc Res 2010;86:82–91.
17. Harrison C, Yang C, Jindal A, DeBerardinis RJ, Hooshyar MA, Merritt M, Dean Sherry A, Malloy CR. Comparison of kinetic models for analysis of pyruvate-to-lactate exchange by hyperpolarized 13 C NMR. NMR Biomed 2012;25:1286–1294.
18. Kazan SM, Reynolds S, Kennerley A, Wholey E, Bluff JE, Berwick J, Cunningham VJ, Paley MN, Tozer GM. Kinetic modeling of hyperpolarized (13) C pyruvate metabolism in tumors using a measured arterial input function. Magn Reson Med 2013;70:943–953.
19. Bohndiek SE, Kettunen MI, Hu DE, Kennedy BW, Boren J, Gallagher FA, Brindle KM. Hyperpolarized [1–13C]-ascorbic and dehydroascorbic acid: vitamin C as a probe for imaging redox status in vivo. J Am Chem Soc 2011;133:11795–11801.
20. Keshari KR, Kurhanewicz J, Bok R, Larson PE, Vigneron DB, Wilson DM. Hyperpolarized 13C dehydroascorbate as an endogenous redox sensor for in vivo metabolic imaging. Proc Natl Acad Sci USA 2011;108:18606–18611.
21. Bastiaansen J, Cheng T, Mishkovsky M, das Neves Duarte J, Comment A, et al. In vivo enzymatic activity of acetylCoA synthetase in skeletal muscle revealed by (13)C turnover from hyperpolarized [1-(13)C]acetate to [1-(13)C]acetylcarnitine. Biochim Biophys Acta 2013;1830:4171–4178.
22. Cummings JH. Short chain fatty acids in the human colon. Gut 1981;22:763–779.
23. Cook SI, Sellin JH. Review article: short chain fatty acids in health and disease. Aliment Pharmacol Ther 1998;12:499–507.
24. Blouin JM, Penot G, Collinet M, Nacfer M, Forest C, Laurent-Puig P, Coumoul X, Barouki R, Benelli C, Bortoli S. Butyrate elicits a metabolic switch in human colon cancer cells by targeting the pyruvate dehydrogenase complex. Int J Cancer 2011;128:2591–2601.
25. Leschelle X, Delpal S, Goubern M, Blottiere HM, Blachier F. Butyrate metabolism upstream and downstream acetyl-CoA synthesis and growth control of human colon carcinoma cells. Eur J Biochem 2000;267:6435–6442.
26. Hadjiagapiou C, Schmidt L, Dudeja PK, Layden TJ, Ramaswamy K. Mechanism(s) of butyrate transport in Caco-2 cells: role of monocarboxylate transporter 1. Am J Physiol Gastrointest Liver Physiol 2000;279:G775–G780.
27. Lorber V, Cook M. The metabolism of n-butyrate-C14 by mammalian heart muscle. J Biol Chem 1955;215:823–832.
28. Roediger WE. The colonic epithelium in ulcerative colitis: an energy-deficiency disease? Lancet 1980;2:712–715.
29. Nilsson AC, Ostman EM, Knudsen KE, Holst JJ, Bjorck IM. A cereal-based evening meal rich in indigestible carbohydrates increases plasma butyrate the next morning. J Nutr 2010;140:1932–1936.
30. Nilsson AC, Ostman EM, Knudsen KE, Holst JJ, Bjorck IM. Metabolism, hypoxia and the diabetic heart. J Mol Cell Cardiol 2011;50:598–605.
31. Taegtmeyer H, Hems R, Krebs HA. Utilization of energy-providing substrates in the isolated working rat heart. Biochem J 1980;186:701–711.
32. Opie LH, Evans JR, Shipp JC. Effect of fasting on glucose and palmitate metabolism of perfused rat heart. Am J Physiol 1963;205:1203–1208.
33. Shipp JC. Interrelation between carbohydrate and fatty acid metabolism of isolated perfused rat heart. Metabolism 1964;13:852–867.
34. Naressi A, Couturier C, Devos JM, Janssen M, Mangeat C, de Beer R, Graveron-Demilly D. Java-based graphical user interface for the MRUI quantitation package. Magma 2001;12:141–152.
35. Naressi A, Couturier C, Castang I, de Beer R, Graveron-Demilly D. Java-based graphical user interface for MRUI, a software package for quantitation of in vivo/medical magnetic resonance spectroscopy signals. Comput Biol Med 2001;31:269–286.
36. Langendorff O. Untersuchungen am überlebenden Säugetierherzen. Pflüger's Arch Ges Physiol 1895;61:291–331.

37. Cole MA, Murray AJ, Cochlin LE, Heather LC, McAleese S, Knight NS, Sutton E, Jamil AA, Parassol N, Clarke K. A high fat diet increases mitochondrial fatty acid oxidation and uncoupling to decrease efficiency in rat heart. Basic Res Cardiol 2011;106:447–457.
38. Heather LC, Catchpole AF, Stuckey DJ, Cole MA, Carr CA, Clarke K. Isoproterenol induces in vivo functional and metabolic abnormalities: similar to those found in the infarcted rat heart. J Physiol Pharmacol 2009;60:31–39.
39. Heather LC, Cole MA, Lygate CA, Evans RD, Stuckey DJ, Murray AJ, Neubauer S, Clarke K. Fatty acid transporter levels and palmitate oxidation rate correlate with ejection fraction in the infarcted rat heart. Cardiovasc Res 2006;72:430–437.
40. Tyler DJ, Lopez O, Cole MA, Carr CA, Stuckey DJ, Lakatta E, Clarke K, Spencer RG. Ongoing dual-angle measurements for the correction of partial saturation in 31P MR spectroscopy. Magn Reson Med 2010;64:957–966.
41. Schneider JE, Cassidy PJ, Lygate C, Tyler DJ, Wiesmann F, Grieve SM, Hulbert K, Clarke K, Neubauer S. Fast, high-resolution in vivo cine magnetic resonance imaging in normal and failing mouse hearts on a vertical 11.7 T system. J Magn Reson Imaging 2003;18:691–701.
42. Tyler DJ, Lygate CA, Schneider JE, Cassidy PJ, Neubauer S, Clarke K. CINE-MR imaging of the normal and infarcted rat heart using an 11.7 T vertical bore MR system. J Cardiovasc Magn Reson 2006;8:327–333.
43. Cassidy PJ, Schneider JE, Grieve SM, Lygate C, Neubauer S, Clarke K. Assessment of motion gating strategies for mouse magnetic resonance at high magnetic fields. J Magn Reson Imaging 2004;19:229–237.
44. Schroeder MA, Atherton HJ, Heather LC, Griffin JL, Clarke K, Radda GK, Tyler DJ. Determining the in vivo regulation of cardiac pyruvate dehydrogenase based on label flux from hyperpolarised [1–13C]pyruvate. NMR Biomed 2011;24:980–987.
45. Dodd MS, Ball V, Bray R, Ashrafian H, Watkins H, Clarke K, Tyler DJ. In vivo mouse cardiac hyperpolarized magnetic resonance spectroscopy. J Cardiovasc Magn Reson 2013;15:19.
46. Atherton HJ, Schroeder MA, Dodd MS, et al. Validation of the in vivo assessment of pyruvate dehydrogenase activity using hyperpolarised 13C MRS. NMR Biomed 2011;24:201–208.
47. Le Belle JE, Harris NG, Williams SR, Bhakoo KK. A comparison of cell and tissue extraction techniques using high-resolution 1H-NMR spectroscopy. NMR Biomed 2002;15:37–44.
48. Allouche-Arnon H, Wade T, Waldner LF, Miller VN, Gomori JM, Katz-Brull R, McKenzie CA. In vivo magnetic resonance imaging of glucose—initial experience. Contrast Media Mol I 2013;8:72–82.
49. Kerbey AL, Randle PJ, Cooper RH, Whitehouse S, Pask HT, Denton RM. Regulation of pyruvate dehydrogenase in rat heart. Mechanism of regulation of proportions of dephosphorylated and phosphorylated enzyme by oxidation of fatty acids and ketone bodies and of effects of diabetes: role of coenzyme A, acetyl-coenzyme A and reduced and oxidized nicotinamide-adenine dinucleotide. Biochem J 1976;154: 327–348.
50. Moreno KX, Sabelhaus SM, Merritt ME, Sherry AD, Malloy CR. Competition of pyruvate with physiological substrates for oxidation by the heart: implications for studies with hyperpolarized [1–13C]pyruvate. Am J Physiol Heart Circ Physiol 2010;298:H1556–H1564.
51. Kunau WH, Dommes V, Schulz H. beta-oxidation of fatty acids in mitochondria, peroxisomes, and bacteria: a century of continued progress. Prog Lipid Res 1995;34:267–342.